

# A Unified Multi-Scale Attention-Based Network for Automatic 3D Segmentation of Lung Parenchyma & Nodules In Thoracic CT Images

Muhammad Abdullah, Furqan Shaukat\*

Faculty of Electrical and Electronics Engineering, University of Engineering and  
Technology Taxila, Pakistan  
furqan.shoukat@uettaxila.edu.pk

**Abstract.** Lung cancer has been one of the major threats across the world with the highest mortalities. Computer-aided detection (CAD) can help in early detection and thus can help increase the survival rate. Accurate lung parenchyma segmentation (to include the juxta-pleural nodules) and lung nodule segmentation, the primary symptom of lung cancer, play a crucial role in the overall accuracy of the Lung CAD pipeline. Lung nodule segmentation is quite challenging because of the diverse nodule types and other inhibit structures present within the lung lobes. Traditional machine/deep learning methods suffer from generalization and robustness. Recent Vision Language Models/Foundation Models perform well on the anatomical level, but they suffer on fine-grained segmentation tasks, and their semi-automatic nature limits their effectiveness in real-time clinical scenarios. In this paper, we propose a novel, fully automatic method for accurate 3D segmentation of lung parenchyma and lung nodules. The proposed architecture is an attention-based, fully convolutional UNet with residual blocks at each encoder-decoder state. Max pooling is replaced by strided convolutions at the encoder, and trilinear interpolation is replaced by transposed convolutions at the decoder to maximize the number of learnable parameters. Dilated convolutions at each encoder-decoder stage allow the model to capture the larger context without increasing computational costs. Increasing the depth of the residual block at each stage helps in learning the complex patterns and fine details in the dataset. The proposed method has been evaluated extensively on one of the largest publicly available datasets, namely LUNA16, and is compared with recent notable work in the domain using standard performance metrics like Dice score, IOU, etc. It can be seen from the results that the proposed method achieves better performance than state-of-the-art methods. The source code, datasets, and pre-processed data can be accessed using the link: <https://github.com/EMeRALDsNRPU/Attention-Based-3D-ResUNet>.

**Keywords:** Lung Nodule Segmentation · Lung Parenchyma Segmentation · Computer Aided Detection · Lung Cancer.

## 1 Introduction

Lung cancer ranks among the most prevalent cancers globally, with around 2.2 million new cases recorded in 2020[28]. The American Cancer Society estimated almost 234,580 new cases of lung cancer in the US for the year 2024 only. Approximately 340 people die because of lung cancer daily in the US, nearly 2.5 times the fatalities attributed to colorectal cancer (CRC), which ranks second in cancer mortality[26]. A survey by the European Society for Medical Oncology (ESMO)[17], suggests that the highest prevalence of lung cancer occurs in Central/Eastern European and Asian populations. The situation in developing countries (such as in Asia) is particularly dire[15]. Research indicates that early detection of lung nodules can significantly improve the survival rate [27]. However, early detection of lung cancer is difficult primarily because of 1) the absence of early symptoms in the majority of patients. 2) a substantial volume of data available in the form of computed tomography (CT) scans, and 3) the inter-observer variability in nodule detection. Computer-aided detection (CAD) can facilitate the early detection of lung nodules and decrease the workload of expert personnel. Lung nodules are typically characterized as the primary symptom of lung cancer, developing within and at the peripheries of the lungs. In radiology, CAD systems can help clinicians in medical image analysis[25] to detect and localize structures of interest in a semi-automatic or fully automated manner. The five-year survival rate for lung cancer patients is the lowest among all cancers, indicating a pressing need for the development of automated and reliable systems to enhance early detection, diagnosis, and treatment. Accurate segmentation of lung parenchyma & lung nodules plays a crucial role in the overall accuracy of the lung CAD pipeline where accurate segmentation of lung lobes ensures the inclusion of juxta-pleural nodules. Lung Nodule segmentation has its own challenges because of the diverse nodule types and other inhibit structures present within the lung lobes. Extensive research has been conducted on the development of lung nodule segmentation systems utilizing traditional machine learning and deep learning methodologies[31, 18, 8, 12, 5, 2, 21, 6]. However, traditional machine learning or deep learning methods suffer from generalization and robustness.

The recent emergence of massive visual language models (VLMs) and their ability to generalize to unseen tasks has prompted the healthcare community to adapt them for numerous medical applications. The Segment Anything Model (SAM) [11] has excelled in various segmentation tasks using standard real-world images. The domain gap between real-world and medical images, such as those in radiology, and its adaptability have been examined in several variants of SAM [13, 19, 9, 23, 24]. Nevertheless, these models have primarily been investigated at the anatomical level, while lesion-level detection remains a challenge because of the fine-grained segmentation nature. In addition, the semi-automatic nature of these VLMs limits their application in real-time clinical scenarios. To this end, we present a novel fully automatic method for accurate 3D segmentation of lung parenchyma and lung nodules. Our **contributions** in this work can be summarized as follows:

- Development of a fully automatic multi-scale attention network for automatic 3D segmentation of lung parenchyma and nodules.
- Proposing a fully convolutional resUnet by replacing the max-pooling with strided convolutions at the encoder and trilinear interpolation by transposed convolutions at the decoder, which maximizes the number of learnable parameters.
- Adapted dilated convolutions at each encoder-decoder stage which allows the model to capture the larger context without increasing any computational cost.
- Increasing the depth of the residual block at each stage thus easing the process of learning the complex patterns and fine details in the dataset.

## 2 Methodology

### 2.1 Dataset curation and Preprocessing

The LUNA dataset[22] is utilized for training and validation of the proposed model. LUNA is a subset of the LIDC-IDRI dataset[4] which contains 1018 CT (Computed Tomography) scans annotated by four expert radiologists in double-blinded fashion. In LUNA, the inconsistent cases have been removed from the original dataset resulting in a total of 888 scans. The nodule inclusion criteria of LUNA have been followed in subsequent nodules’ evaluations which gives a total of 1186 nodules. The corresponding lung masks are also given, which are used as labels for training the proposed model for lung segmentation. Nodule masks are taken from the original LIDC-IDRI dataset of respective cases, which are used as labels for training the proposed model for nodule segmentation.

Each scan of a 3D CT image and corresponding label is resized to  $300 \times 300$  for lung segmentation and  $256 \times 256$  for nodule segmentation. For lung lobe segmentation, after resizing, immediate 11 scans around each side of the median slice were taken, thus making a total of 23 slices (11+11+median slice). For lung nodule segmentation, all the slices of nodule appearance were considered. This cropping was performed because most image information is contained around the median slice. In short, resizing and cropping help manage the variables in memory.

### 2.2 Network architecture

We have taken UNet[20] as a backbone of our proposed model with 4 encoder and decoder stages as shown in Figure 1. A bottleneck is used after the last encoder stage and before the first decoder stage. Each encoder-decoder stage and bottleneck contains a Residual block, which is shown in Figure 2. Furthermore, Transposed convolution (stride=2) is utilized at each decoder stage for upsampling, which replaces the trilinear interpolation, thus increasing the number of learnable parameters. Attention gates are utilized between the last encoder stage ( $e4$ ) and the first decoder stage ( $d4$ ). Similarly ( $e3, d3$ ), ( $e2, d2$ ), and ( $e1, d1$ ) pairs

serve as inputs to the attention gates. The working of an attention gate is shown in Figure 3. The result of the attention gate at each stage is concatenated with the decoder output after passing the output from a 3D convolution. The Concatenation operation is defined as:

$$\text{CAT} = \text{cat}(A, D_i), \quad \text{where } i = 4, \dots, 1 \quad (1)$$

where:

- $A$  represents the attention gate.
- $D_i$  is the output of the decoder after passing through 3D convolution.

The result of concatenation passes to the decoder b for further processing of concatenated features. The output features of decoder b pass to next decoder as input after upsampling by transposed convolution. The final output after the last concatenation operation passes through a 3D convolution and a cropping operation. Similarly, two additional convolutional operations are applied to mitigate the effect of cropping. Finally, the sigmoid function is applied to predict the binary output. For nodule segmentation extra cropping layers were removed which can cause the model to memorize the patterns thus decreasing the efficiency and generalization of the proposed architecture. Similarly, decoder b stages were also removed to prevent the overfitting which could arise due to complex nature of the network.

### 2.3 Residual block

Our proposed residual block is inspired by [10] with certain modifications. The modified 3D Residual block contains 2 layers of operations, with each layer containing  $3 \times 3$ , 3D convolution (with stride 2 at the encoder and stride 1 at the decoder), and 3D Batch normalization. Sride 2 convolution replaces the max-pooling operation, thus increasing the number of learnable parameters. Similarly, dilation of 2 is utilized at each 3D convolution. The dilated convolutions proposed in [29], which are applied at each stage, expand the receptive field of the deep network without increasing the computational cost. Batch normalization helps in the fast convergence of the model while training. ReLU activation is applied after the first layer and the skip connection, which brings non-linearity to the model. Increasing the depth of the residual block helps in learning the fine details and complex patterns in the dataset. The output of the residual block is shown as:

$$\text{Out} = \sigma(x + f(x)) \quad (2)$$

where:

$x$  is input.

$f(x)$  is output after two layers of residual block.

$\sigma$  is ReLU activation.

For nodule segmentation Batch normalization was replaced by Group normalization, which works better with small batch sizes. Similarly, multi-head attention was introduced in the residual block which can capture different type of relationships simultaneously, thus making the model dual attention network.

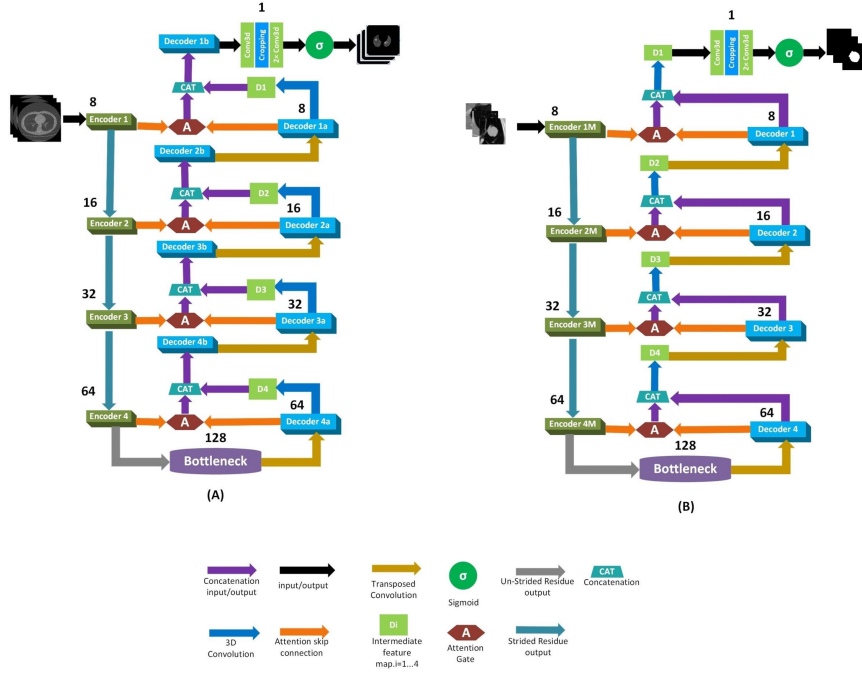


**Fig. 1.** Block diagram of the proposed architecture. Each encoder shown as green and each decoder, shown as light blue is the residual block. Number of channels are mentioned above each encoder/decoder block. (A) Proposed Lung segmentation Network. (B) Proposed Nodule segmentation network.

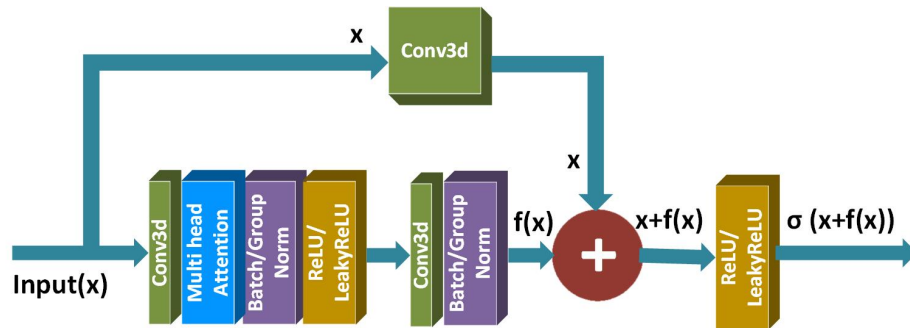


**Fig. 2.** Proposed 3D residual block with dilated convolutions.

## 2.4 Attention Gates

The concept of an attention gate proposed by [16] is extended to 3D in our proposed scheme. Three-dimensional (3D) attention gates with dilated convolutions (i.e., dilation = 2) used in our proposed scheme are shown in Figure 3. Two additional 3D transposed convolutions (stride =2) and 3D convolutions were added before the addition and multiplication of feature maps to bring depth in attention gates and hence more robust features are learnt. The output  $z_0$  is a 1-channel feature map, which is multiplied with the transformed input  $f_t(x)$  to get the attention output  $z$ . The input signal is the encoder output, and the gating signal is the decoder output of each stage. For nodule segmentation Group

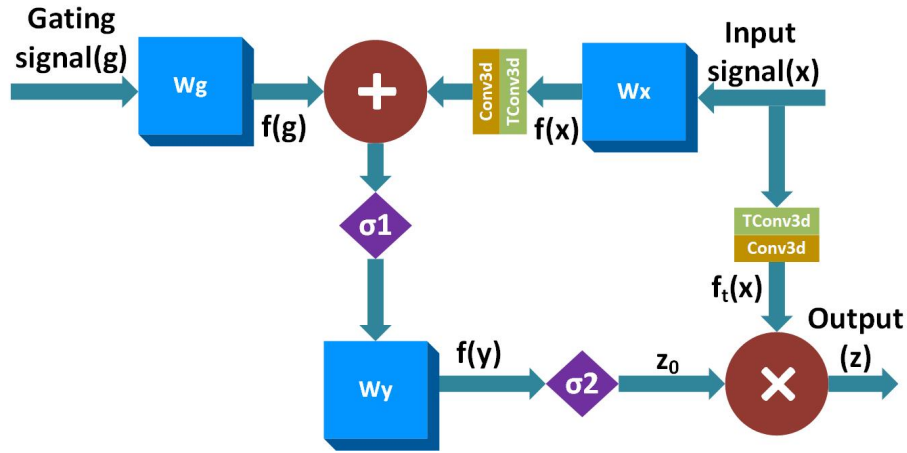


**Fig. 3.** Proposed 3D Attention Gate with dilated convolutions. Dilated convolution operations are shown as  $W_x$ ,  $W_g$  and  $W_y$ .  $\sigma_1$  and  $\sigma_2$  show the ReLU and Sigmoid activations, respectively. Addition and multiplication of feature maps are shown by  $+$  and  $\times$  respectively. TConv3D and Conv3D are transposed 3D strided convolutions and 3D convolutions, respectively.

normalization was added after each convolutional layer of the attention gate, which help in achieving fast convergence.

## 2.5 Loss function

The loss function utilized for lung and nodule segmentation is a combination of Binary cross-entropy and Dice loss. Binary cross-entropy and Dice loss are robust in nature and are widely adapted in medical image segmentation tasks. Binary cross entropy is defined as:

$$L_{BCE} = -\frac{1}{N} \sum_{i=1}^N [m_i \log p_i + (1 - m_i) \log(1 - p_i)], \quad (3)$$

Similarly, Dice loss is defined as:

$$L_{Dice} = 1 - \frac{2 \sum_{i=1}^N m_i p_i}{\sum_{i=1}^N (m_i)^2 + \sum_{i=1}^N (p_i)^2}, \quad (4)$$

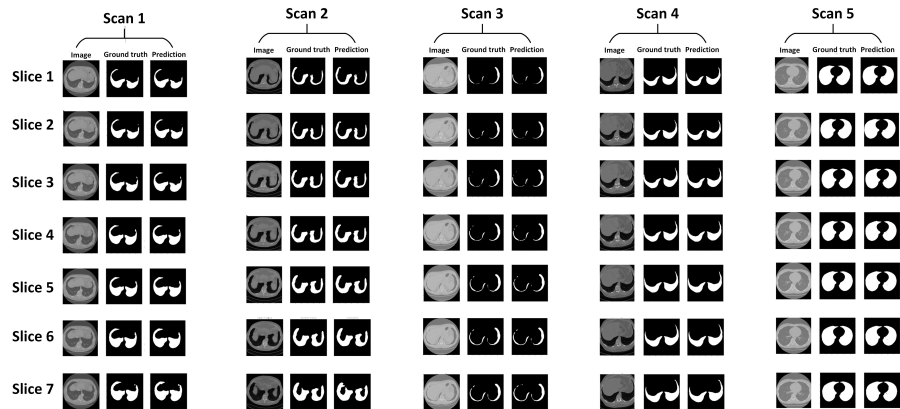
The final loss L is defined by

$$L = L_{BCE} + L_{Dice}, \quad (5)$$

### 3 Experimental Results and Discussion.

The LUNA 16[22] dataset was used for training and validation purposes. The dataset was split into the train, validation, and test sets with a ratio of 60-20-20, respectively. The proposed network was trained separately for lung parenchyma segmentation and nodule segmentation. A total of 100 epochs were used in both cases. A batch size of 01 was selected due to the limited memory used to handle large arrays. The loss function was minimized using the Adam optimizer with a learning rate of 1e-4. A small learning rate improves the generalizability of the model and helps in learning complex patterns in the dataset. The trained model was tested on the 20% test dataset, which was never seen by the model during training. The proposed model was evaluated for both tasks, i.e., lung parenchyma segmentation and lung nodule segmentation, using standard performance metrics like Dice Score, IOU, Precision, and Recall, and was compared with other notable work in the domain. However, we would like to emphasize that most of the techniques were optimized for only one task i.e., either lung parenchyma or lung nodule segmentation, whereas we have used the same architecture for both tasks, which reflects the ability of the proposed model to better generalize to different scales of segmentation. The results are presented in Tables 1 and 2, where Table 1 represents lung parenchyma segmentation and Table 2 represents lung nodule segmentation results. We have tried to include the state of the art and recent studies in our comparison. For lung parenchyma segmentation, the test results of the recent studies [31, 18, 8] and results of SOTA like UNet, AttentionUNet, and DeepLabV1 reported by [8], along with ours, are shown in Table 1 for comparison. Similarly, for lung nodule segmentation, test results of the recent studies [31, 18, 8] along with ours are shown in Table 2 for comparison. It can be seen from both tables that our proposed method outperforms the other studies in lung segmentation tasks, even though our method is evaluated on a considerably large and well-established dataset as compared to other techniques, and performs satisfactorily for nodule segmentation. However, we would like to note that a 3D crop of the size  $64 \times 64 \times 64$  of a CT scan was used as input to the nodule segmentation model. As this cropping decreases the context for the 3D nodule, a fall in dice score and IoU is observed. These results can be further improved by considering the larger cropped image size, which will provide more information around the lung nodule and help the model better understand the CT image in a broader context. For qualitative comparison, we have included the sample results of both tasks as shown in Fig. 4 and Fig. 5, respectively.

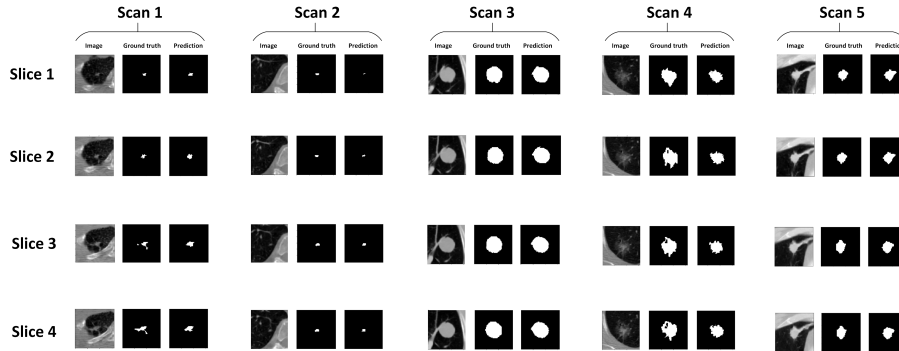
Figure 4 shows the inference results of the proposed model for lung parenchyma segmentation, and Figure 5 shows the inference results for lung nodule segmentation. It can be seen that the model performs quite well on both tasks. Some other comparable works with respect to architecture for these two tasks are [14, 1, 3, 5, 30]. However, we have added the following incremental novelties to our proposed architecture to improve its performance and generalization ability. 3D attention gates and residual blocks have been used compared to 2D used in [14]. Similarly, the proposed architecture uses 3D fully convolutional layers instead of max pooling and  $3 \times 3$  transposed convolutions at the decoder stage. Agarwala et al.[1] uses 3D UNet, but single encoded-decoder blocks utilize simple 3D convolutional blocks without Residual connections. Our proposed Residual block not only utilizes skip connections but has  $2 \times$  increased depth. SAA-UNet [3] proposed by Alshomrani et al. has a similar 2D architecture, but residual connections were not utilized at single encoder-decoder stages. MRUNet-3D[5] is also a comparable architecture but lacks the attention gates. Our model also replaces the trilinear interpolation with transposed convolutions, which increases the number of learnable parameters. AGs-UNet, proposed by Yu et al. [30], lacks batch normalization at each stage, which is essential for fast convergence. Furthermore, our proposed model utilizes the dilated convolution at each stage, which expands the receptive field of the deep network without increasing any computational cost. An expanded receptive field allows the model to capture a broader context in an image.



**Fig. 4.** Sample results of lung parenchyma segmentation. The first column of each scan represents different slices, the second column represents the ground truth and third column represents the segmentation results

**Table 1.** Comparison of Lung Parenchyma Segmentation Results with Existing Methods.

| Author                 | Year | Method                                       | No. of samples    | Dice Score (%) | IoU (%)      | Precision (%) | Recall (%) |
|------------------------|------|--|-------------------|----------------|--------------|---------------|------------|
| Ronneberger et al.[20] | 2015 | UNet   | 163 CT Scans      | 91.52          | 84.73        | -             | -          |
| Chen et al.[7]         | 2017 | DeepLabV1                                    | 163 CT Scans      | 88.67          | 80.77        | -             | -          |
| Oktay et al.[16]       | 2018 | AttentionUNet                                | 163 CT Scans      | 91.96          | 86.48        | -             | -          |
| Zhang et al.[31]       | 2023 | NASNet-large Net                             | 1000 X-Ray Images | 92.00          | 87.00        | -             | -          |
| Poonkodi et al.[18]    | 2023 | MSCAUNet-3D                                  | 335 CT Scans      | 91.40          | 90.40        | -             | -          |
| Gang et al.[8]         | 2024 | Pyramidal Pooling Channel Transformer (PPCT) | 163 CT Scans      | 88.99          | 80.40        | 88.13         | -          |
| <b>Ours</b>            | 2025 | 3D-Attention ResUNet                         | 888 CT Scans      | <b>93.61</b>   | <b>91.03</b> | 88.72         | 88.64      |

**Fig. 5.** Sample results of lung nodule segmentation. The first column of each scan represents different slices, the second column represents the ground truth and third column represents the segmentation results

**Table 2.** Comparison of Lung Nodule Segmentation Results with Existing Methods.

| Author               | Year | Method                                     | No. of samples | Dice Score (%) | IoU (%) | Precision (%) | Recall (%) |
|----------------------|------|--|----------------|----------------|---------|---------------|------------|
| Bbosa et al.[5]      | 2024 | MRUNet-3D                                  | 888 CT Scans   | 83.47          | 86.27   | 83.39         | -          |
| Agnes et al.[2]      | 2024 | Wavelet U-Net++                            | 1018 CT Scans  | 93.70          | 87.80   | -             | -          |
| Selvadass et al.[21] | 2024 | SAtUNet                                    | 1018 CT Scans  | 81.10          | 72.24   | 90.87         | 84.22      |
| Cai et al.[6]        | 2024 | MDFN: A Multi-level Dynamic Fusion Network | 888 CT Scans   | 89.19          | 80.78   | -             | 88.89      |
| <b>Ours</b>          | 2025 | 3D-Attention ResUNet                       | 888 CT Scans   | 80.83          | 68.29   | 78.90         | 83.95      |

## 4 Conclusions

In this paper, we present a fully automatic 3D lung parenchyma and lung nodule segmentation network. The proposed architecture is attention-based fully convolutional UNet with residual blocks at each encoder-decoder state. Maxpooling is replaced by strided convolutions at the encoder and trilinear interpolation is replaced by transposed convolutions at the decoder to maximize the number of learnable parameters. Dilated convolutions at each encoder-decoder stage allow the model to capture the larger context without increasing computational costs. Increasing the depth of residual block at each stage helps in learning the complex patterns and fine details in the dataset. One of the largest publicly available datasets, LUNA16, is used for model training and validation. The proposed method is compared with state-of-the-art methods using the standard performance metrics, exhibiting superior performance as compared to its counterparts. The proposed method can be integrated into an end-to-end pipeline for lung nodule detection and its subsequent characterization. The proposed method can be used for early lung cancer screening and assist the medical community in the early diagnosis of lung cancer.

**Acknowledgments.** This work is part of the NRPU project # 17019 entitled “EMeR-ALDS: Electronic Medical Records driven Automated Lung nodule Detection and cancer risk Stratification” funded by Higher Education Commission of Pakistan.

**Disclosure of Interests.** The authors have no competing interests to declare that are relevant to the content of this article.

## References

1. Agarwala, S., Sharma, S., Shankar, B.U.: A-unet: Attention 3d unet architecture for multiclass segmentation of brain tumor. In: 2022 IEEE Region 10 Symposium (TENSYPMP). pp. 1–5. IEEE (2022)
2. Agnes, S.A., Solomon, A.A., Karthick, K.: Wavelet u-net++ for accurate lung nodule segmentation in ct scans: Improving early detection and diagnosis of lung cancer. *Biomedical Signal Processing and Control* **87**, 105509 (2024)
3. Alshomrani, S., Arif, M., Al Ghamdi, M.A.: Saa-unet: Spatial attention and attention gate unet for covid-19 pneumonia segmentation from computed tomography. *Diagnostics* **13**(9), 1658 (2023)
4. Armato III, S.G., McLennan, G., Bidaut, L., McNitt-Gray, M.F., Meyer, C.R., Reeves, A.P., Zhao, B., Aberle, D.R., Henschke, C.I., Hoffman, E.A., et al.: The lung image database consortium (lidc) and image database resource initiative (idri): a completed reference database of lung nodules on ct scans. *Medical physics* **38**(2), 915–931 (2011)
5. Bbosa, R., Gui, H., Luo, F., Liu, F., Efiio-Akolly, K., Chen, Y.P.P.: Mrunet-3d: A multi-stride residual 3d unet for lung nodule segmentation. *Methods* **226**, 89–101 (2024)
6. Cai, Y., Liu, Z., Zhang, Y., Yang, Z.: Mdfn: A multi-level dynamic fusion network with self-calibrated edge enhancement for lung nodule segmentation. *Biomedical Signal Processing and Control* **87**, 105507 (2024)
7. Chen, L.C., Papandreou, G., Kokkinos, I., Murphy, K., Yuille, A.L.: Deeplab: Semantic image segmentation with deep convolutional nets, atrous convolution, and fully connected crfs. *IEEE transactions on pattern analysis and machine intelligence* **40**(4), 834–848 (2017)
8. Gang, L., Zhichao, L., Ling, Z., Guijuan, C., Kairu, Z., Rui, L.: Segmentation algorithm for honeycomb lung ct images based on pyramidal pooling channel transformer. *Applied Soft Computing* p. 112557 (2024)
9. Gong, S., Zhong, Y., Ma, W., Li, J., Wang, Z., Zhang, J., Heng, P.A., Dou, Q.: 3dsam-adapter: Holistic adaptation of sam from 2d to 3d for promptable medical image segmentation. *arXiv preprint arXiv:2306.13465* (2023)
10. He, K., Zhang, X., Ren, S., Sun, J.: Deep residual learning for image recognition. In: *Proceedings of the IEEE conference on computer vision and pattern recognition*. pp. 770–778 (2016)
11. Kirillov, A., Mintun, E., Ravi, N., Mao, H., Rolland, C., Gustafson, L., Xiao, T., Whitehead, S., Berg, A.C., Lo, W.Y., et al.: Segment anything. *arXiv preprint arXiv:2304.02643* (2023)
12. Lu, F., Zhang, Z., Liu, T., Tang, C., Bai, H., Zhai, G., Chen, J., Wu, X.: A weakly supervised inpainting-based learning method for lung ct image segmentation. *Pattern Recognition* **144**, 109861 (2023)
13. Ma, J., He, Y., Li, F., Han, L., You, C., Wang, B.: Segment anything in medical images. *Nature Communications* **15**(1), 654 (2024)
14. Maji, D., Sigedar, P., Singh, M.: Attention res-unet with guided decoder for semantic segmentation of brain tumors. *Biomedical Signal Processing and Control* **71**, 103077 (2022)

15. Moore, M.A., Attasara, P., Khuhaprema, T., Le, T., Nguyen, T., Raingsey, P.P., Sriamporn, S., Sriplung, H., Srivanatanakul, P., Bui, D., et al.: Cancer epidemiology in mainland south-east asia-past, present and future. *Asian Pac J Cancer Prev* **11**(Suppl 2), 67–80 (2010)
16. Oktay, O., Schlemper, J., Folgoc, L.L., Lee, M., Heinrich, M., Misawa, K., Mori, K., McDonagh, S., Hammerla, N.Y., Kainz, B., et al.: Attention u-net: Learning where to look for the pancreas. *arXiv preprint arXiv:1804.03999* (2018)
17. Planchard, D., Popat, S., Kerr, K., Novello, S., Smit, E., Faivre-Finn, C., Mok, T., Reck, M., Van Schil, P., Hellmann, M., et al.: Metastatic non-small cell lung cancer: Esmo clinical practice guidelines for diagnosis, treatment and follow-up. *Annals of Oncology* **29**, iv192–iv237 (2018)
18. Poonkodi, S., Kanchana, M.: Mscaunet-3d: Multiscale spatial channel attention 3d-unet for lung carcinoma segmentation on ct image. In: 2023 International Conference on Advances in Intelligent Computing and Applications (AICAPS). pp. 1–5. IEEE (2023)
19. Qiu, Z., Hu, Y., Li, H., Liu, J.: Learnable ophthalmology sam. *arXiv preprint arXiv:2304.13425* (2023)
20. Ronneberger, O., Fischer, P., Brox, T.: U-net: Convolutional networks for biomedical image segmentation. In: Medical image computing and computer-assisted intervention—MICCAI 2015: 18th international conference, Munich, Germany, October 5–9, 2015, proceedings, part III 18. pp. 234–241. Springer (2015)
21. Selvadass, S., Bruntha, P.M., Sagayam, K.M., Günerhan, H.: Satunet: Series atrous convolution enhanced u-net for lung nodule segmentation. *International Journal of Imaging Systems and Technology* **34**(1), e22964 (2024)
22. Setio, A.A.A., Traverso, A., De Bel, T., Berens, M.S., Van Den Bogaard, C., Cerello, P., Chen, H., Dou, Q., Fantacci, M.E., Geurts, B., et al.: Validation, comparison, and combination of algorithms for automatic detection of pulmonary nodules in computed tomography images: the luna16 challenge. *Medical image analysis* **42**, 1–13 (2017)
23. Shaharabany, T., Dahan, A., Giryas, R., Wolf, L.: Autosam: Adapting sam to medical images by overloading the prompt encoder. *arXiv preprint arXiv:2306.06370* (2023)
24. Shaukat, F., Anwar, S.M., Parida, A., Lam, V.K., Linguraru, M.G., Shah, M.: Lung-cadex: Fully automatic zero-shot detection and classification of lung nodules in thoracic ct images. In: International Workshop on Machine Learning in Medical Imaging. pp. 73–82. Springer (2024)
25. Shaukat, F., Raja, G., Frangi, A.F.: Computer-aided detection of lung nodules: a review. *Journal of Medical Imaging* **6**(2), 020901–020901 (2019)
26. Siegel, R.L., Giaquinto, A.N., Jemal, A.: Cancer statistics, 2024. *CA: a cancer journal for clinicians* **74**(1), 12–49 (2024)
27. Siegel, R.L., Miller, K.D., Jemal, A.: Cancer statistics, 2019. *CA: a cancer journal for clinicians* **69**(1), 7–34 (2019)
28. Sung, H., Ferlay, J., Siegel, R.L., Laversanne, M., Soerjomataram, I., Jemal, A., Bray, F.: Global cancer statistics 2020: Globocan estimates of incidence and mortality worldwide for 36 cancers in 185 countries. *CA: a cancer journal for clinicians* **71**(3), 209–249 (2021)
29. Yu, F.: Multi-scale context aggregation by dilated convolutions. *arXiv preprint arXiv:1511.07122* (2015)
30. Yu, M., Chen, X., Zhang, W., Liu, Y.: Ags-unet: Building extraction model for high resolution remote sensing images based on attention gates u network. *Sensors* **22**(8), 2932 (2022)

31. Zhang, Y.: Lung segmentation with nasnet-large-decoder net. arXiv preprint arXiv:2303.10315 (2023)